Paper

HEATING AND PAIN SENSATION PRODUCED IN HUMAN SKIN BY MILLIMETER WAVES: COMPARISON TO A SIMPLE THERMAL MODEL

Thomas J. Walters,* Dennis W. Blick,* Leland R. Johnson,† Eleanor R. Adair,† and Kenneth R. Foster‡

Abstract—**Cutaneous thresholds for thermal pain were measured in 10 human subjects during 3-s exposures at 94 GHz continuous wave microwave energy at intensities up to ≈ 1.8 W cm^{-2}. During each exposure, the temperature increase at the skin's surface was measured by infrared thermography. The mean (± s.e.m.) baseline temperature of the skin was 34.0 ± 0.2°C. The threshold for pricking pain was 43.9 ± 0.7°C, which corresponded to an increase in surface temperature of ≈ 9.9°C (from 34.0°C to 43.9°C). The measured increases in surface temperature were in good agreement with a simple thermal model that accounted for heat conduction and for the penetration depth of the microwave energy into tissue. Taken together, these results support the use of the model for predicting thresholds of thermal pain at other millimeter wave (length) frequencies.**

Health Phys. 78(3):259–267; 2000

Key words: skin dose; radiofrequency; radiation, nonionizing; microwaves

INTRODUCTION

Exposure to radiofrequency radiation (RFR) at sufficiently high intensities produces perceptible increases in tissue temperature. Indeed, the first line of defense against overexposure to RF energy, as to any source of heat, is the prompt sensation of warmth and/or pain. At microwave frequencies above 10 GHz, the energy penetration depth is small (not more than a few millimeters or less) and the heating takes place near the surface of the skin. Because of the increasing use of such energy, sometimes at high power levels, it is becoming ever more important to identify the limits of safe exposure with respect to thermal hazards.

* Veridian Engineering, Inc., P.O. Box 35505, Brooks Air Force Base, TX 78235; † AFRL/Directed Energy, Bioeffects Division, 8308 Hawks Road, Brooks AFB, TX 78235; ‡ Department of Bioengineering, University of Pennsylvania, 220 S. 33rd Street, Philadelphia, PA 19104-6392.

For correspondence or reprints contact: T. J. Walters, Veridian Engineering, Inc., P.O. Box 35505, Brooks Air Force Base, TX 78235, or email at thomas.walters@aloer.brooks.af.mil.

(*Manuscript received* 6 *April* 1999; *revised manuscript received* 14 *September* 1999, *accepted* 7 *November* 1999)

0017-9078/00/0

Only limited data are available concerning the thermal responses of humans to microwave energy, and most of those data are for frequencies below 10 GHz. We have measured warmth detection-thresholds across a wide range of microwave frequencies, including millimeter wavelengths, within the same subject population (Blick et al. 1997). We have also shown that these thresholds of sensation can be interpreted as reflecting an increase in surface temperature that is independent of the irradiation frequency (Riu et al. 1997). The use of a standard protocol that incorporated measurements over a broad frequency range enabled us to determine the importance of energy-penetration depth both to sensation and to the underlying cutaneous events.

The threshold for thermal pain has been determined for microwave (3 GHz; Cook 1952b) and infrared irradiation (Cook 1952b; Hardy et al. 1952) in human subjects. The threshold for pain was found to be a function of absolute skin temperature and was independent of baseline temperature, duration, intensity, and heating rate for 3 GHz RFR (Cook 1952b) and infrared irradiation (Hardy et al. 1952). Thus, it should be possible to use a thermal model to predict the pain thresholds for microwave energy over a broad range of frequencies and at least short exposure times. Apart from their importance to an understanding of thermal physiology, such data are important for setting human exposure limits, in particular for millimeter waves, where the energy-penetration depth is very small.

The purpose of the present study was threefold: 1) To determine the pain threshold for 94 GHz mm-wave irradiation in human subjects; 2) to extend our earlier observations of the perception threshold for 94 GHz mm-wave irradiation; and 3) to develop a simple thermal model, based on the heat conduction equation, that would allow the accurate prediction of pain at other millimeter-wave frequencies.

MATERIALS AND METHODS

Subjects

The subjects were 3 female and 7 male Caucasian volunteers (military, Department of Defense civilians,

and contractors) involved in research on biological effects of RFR. They ranged in age from 31 to 70 y (43.7 ± 12.3). All subjects were unpaid volunteers who read and signed an informed consent document prior to participation. The use of human subjects in this research was in accordance with a protocol approved by the institutional review board on human use (Brooks Air Force Base, Air Force Research Laboratory Advisory Committee on Human Experimentation), and by the Office of the Surgeon General of the Air Force.

Microwave exposure parameters

A 50-W transmitter manufactured by Applied Electromagnetics, Inc.,[§] with a Varian VKB2462L2 gridded extended oscillator,[‖] emitted microwaves at a frequency of 94 GHz. A gaussian dielectric lens (Shelton 1991) was used to augment the maximal available power density by focusing the output of the transmitter into a beam with a diameter of 4.0 cm. The input side of the lens had a focal length of 90 cm, so the lens was positioned 90 cm from the conical output antenna of the transmitter. The power output (of the transmitter) was set to a maximum that corresponded to an exposure that was estimated to be 10–20% higher than the pain threshold of the least sensitive subject. Varying the duty cycle of a 1 kHz rectangular wave pulse train that gated the output of the transmitter produced steps in power density below this maximum. Pulse durations to produce the required duty cycles (50–90%) were calculated by a computer program and transmitted to a programmable oscillator that produced pulse trains with the required duty cycle and duration (3 s).

Infrared thermography

IR thermography of the irradiated skin was performed using a Radiance 1 Infrared Camera System[¶] equipped with a 50-mm lens. The camera contains a focal plane array composed of 256 × 256 indium antimonide sensors. With the region of interest on the subject's back located 1.5 m from the camera, each sensor measured the temperature of a square patch of skin 500 μm × 500 μm. Images were sampled at a rate of either 4.6 or 8.6 frames per second for an interval containing the stimulus and 1 s before. Automated image analysis was performed off-line using a LabView[#] based program. The program determined the mean, minimal, and maximal value of a 100 mm^2 area of interest (AOI). Multi-point calibration with a Mikron M340 black-body calibration source** provided a measured accuracy of ± 0.1°C over the temperature range examined. The total data set consisted of 180 runs on 8 subjects at 4.6 frames per second and 52 runs on two subjects at 8.6 frames per second.

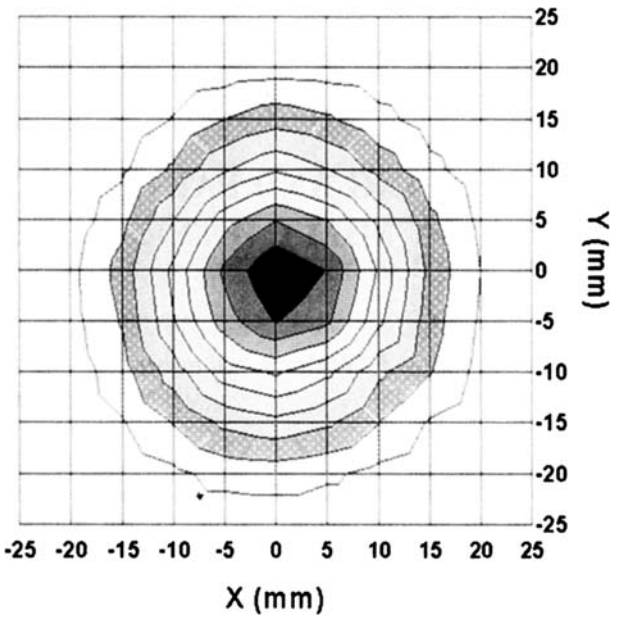

Fig. 1. Field map of the mm-wave field across an x-y plane located 188 cm from the lens. The power sensor was secured to an x-y-z positioner and readings were obtained at 5-mm increments in both the x- and y-coordinates. The central black region represents the peak power density (91–100%), and was the area examined in the present investigation; each surrounding area represents an additional 10% decrement in power density.

Field measurements

A Hewlett Packard power sensor (Model W8486A)[††] attached to an open ended waveguide (Millitech, Model WR10),[‡‡] connected to a Hewlett Packard power meter (Model 437b), was used to map the field at the location of the subject's back. Field mapping was conducted in the x-y plane 188 cm from the lens. The power sensor was secured to an x-y-z positioner (Shelton 1991) and readings were obtained at 5.0-mm increments in both the x- and y-coordinates. A map of the resulting field is shown in Fig. 1. For purposes of specifying the power density of the various stimuli used in the experiment, the mean power density within the 90% contour was used.

Psychophysical technique

A modified staircase procedure (Simpson 1989; Cornsweet 1962) was used to determine the pain threshold. Power density was varied in steps of 50 mW cm^{-2} from 1,750 mW cm^{-2} (which was above the pain threshold for the least sensitive subject) to 900 mW cm^{-2}

[§] Applied Electromagnetics, Inc., 1281 Kennestone Circle, Suite 100, Marietta, GA 30066.

[‖] Varian Canada, Inc., 45 River Drive, Georgetown, Ontario, Canada.

[¶] Amber Engineering, Inc., a Raytheon Systems Company, 6380 Hollister Avenue, Goleta, CA 93117-3179.

[#] National Instruments, Inc., 6504 Bridge Point Pkwy, Austin, TX 78730.

** Mikron Instrument Company, Inc., 16 Thornton Road, Oakland, NJ 07436.

[††] Hewlett-Packard, Co., 14100 San Pedro Avenue, Suite 100, San Antonio, TX 78232.

[‡‡] Millitech, Inc., South Deerfield Research Park, P.O. Box 109, South Deerfield, MA 01373.

(which was below the pain threshold for the most sensitive subject). The stimulus intensity presented on each trial was selected randomly from one of two concurrently operating step series of stimuli. This procedure made the intensity of the next stimulus unpredictable by the subject. The step method presently employed (Simpson 1989) is a variant of older, adaptive staircase methods. It is an efficient means to determine sensory threshold values, because it concentrates stimulus presentations in the region of the threshold so that each presentation (after a brief initial period of "homing in") provides maximal information regarding the threshold. Within each step series, the stimulus level in each trial depended on the responses in previous trials. At a given stimulus level, two consecutive "no" responses (indicating that the subject felt no pain from the exposure in that trial) produced an increase in intensity for the next presentation from that series. A single "yes" response (the subject did feel pain) produced a decrease of intensity in the next trial. Within 32 trials, the two series of steps tended to converge on a stimulus level that evoked "yes" responses one-third of the time. When the responses from the two series were combined, the relative frequency of "yes" responses increased monotonically with intensity, and the 33.3% "yes" point was readily determined by linear interpolation between the two intensities that bracketed this point. The interpolated value was recorded as the threshold for that subject. Due to the statistical nature of the process, this threshold value corresponds to the 29.3% probability of a "yes" response on a standard psychometric function (Wetherill and Levitt 1965). Thus, the step method will yield slightly lower threshold estimates than those based on a 50% "yes" criterion.

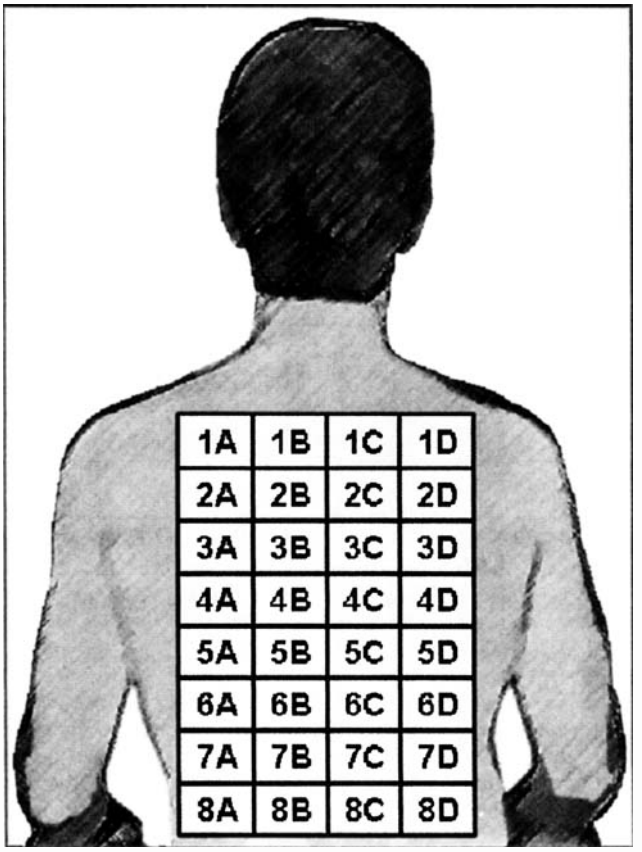

Fig. 2. A grid of the exposure area superimposed over a sketch of a subject's back. Subjects were exposed in the following order: 8C, 8A, 8D, 8B, 4C, 4A, 4D, 4B, 7CADB, 3CADB, 6CADB, 2CADB, 5CADB, 1CADB.

Procedures

Procedures were similar to those previously reported (Blick et al. 1997), except for the duration (3 s), size (4-cm-diameter irradiated area of the skin) and locus of stimulation. To avoid carry-over effects, the 32 stimuli were presented to different positions on the subjects' backs. The lateral and/or vertical position on the subject was changed between each exposure. The changes in vertical and lateral position produced a 4 × 8 rectangular array of stimulus sites. The lateral positions (A through D) were at least 5 cm apart, with two positions on each side of the midline. The vertical positions (1 through 8) were 4 cm apart, with the highest located 14 cm above the seventh thoracic vertebra. Sites in this array were stimulated in the order: 8CADB; 4CADB; 7CADB; 3CADB; 6CADB; 2CADB; 5CADB; and 1CADB, where the number refers to the row (horizontal position) and the letter to the column (vertical position) (Fig. 2). As the intertrial interval was at least 1 min, stimulation of horizontally adjacent sites was separated by at least 2 min, while stimulation of vertically adjacent sites was separated by at least 8 min. The average testing session lasted 35 min.

A schematic diagram of the experimental setup is shown in Fig. 3. An air-conditioning unit circulated air through the subject's chamber at a temperature of 23 ± 0.5°C. Ambient temperature outside the test chamber was maintained at 23 ± 2.5°C. Exposures of 3 s duration occurred at 1–2 min intervals. After each exposure, the subject was required to give a yes-or-no decision regarding whether the stimulus was painful. A warning via intercom was given to the subject 4–6 s prior to each exposure. The subject was visible and audible to the experimenters throughout all experimental sessions via a video monitor and intercom.

Thermal models

Following Cook (1952a) we interpreted the data using a one-dimensional thermal model, based on a solution of the heat conduction equation:

$$k\nabla^2 T(x, t) + Q(x, t) = \rho C \frac{\partial T(x, t)}{\partial t}, \qquad (1)$$

where $T(x,t)$ is the temperature at distance x beneath the surface and time t, C is the specific heat, k is the thermal

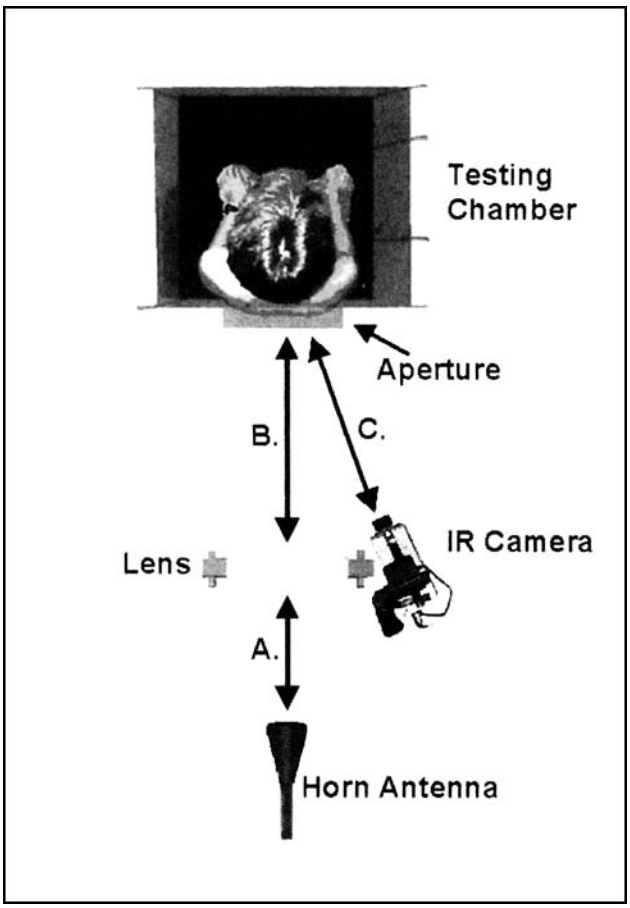

Fig. 3. A schematic diagram of the experimental setup viewed from above. The following distances are: A) 90 cm; B) 188 cm; and C) 190 cm. The dimensions of the exposure chamber were: 90 cm (w) × 90 cm (l) × 180 cm (h).

conductivity, ρ is the density of the tissue, and $Q(x,t)$ is the rate of energy deposition at location x and time t. The rate of energy deposition at a distance x into the tissue is given by eqn (2):

$$Q(x, t) = \frac{I_o T}{L} e^{-x/L}, \qquad (2)$$

where T is the fraction of incident energy that is transmitted into the tissue (the energy transmission coefficient) and L is the distance by which the field intensity has fallen to a factor of $1/e$ just beneath the surface (i.e., the energy-penetration depth) and I_o is the incident power density (i.e., the exposure).

This one-dimensional model strictly applies for a plane surface exposed to a uniform beam of energy. However, in this study the exposures were sufficiently short that heat diffusion along the surface was negligible compared with that perpendicular to the surface; therefore this simple one-dimensional model will suffice.

Assuming insulated boundary conditions (i.e., no heat loss from the skin into space), the solution of eqn (1) for the surface temperature (T_{sur}) is

$$T_{sur}(t) = T_o\left[2\sqrt{\frac{t}{\pi\tau}} + e^{t/\tau} erfc(\sqrt{t/\tau}) - 1\right] \qquad (3)$$

where

$$T_o = \frac{I_o L T}{k}$$

$$\tau = \frac{L^2 \rho C}{k},$$

and $erfc(x)$ is the complementary error function. The thermal time constant τ is the time required for thermal energy to diffuse a distance equal to the energy-penetration depth, and is of the order of 1 s in the present case. For exposure times $> \tau$ the error function becomes very small, and the temperature at the surface grows as the square root of time, which is characteristic of surface heating such as would be produced by infrared heating.

The surface temperature given in eqn (3) is a function of the incident power density, as well as of the thermal and electrical properties of the tissue. We tested the model by fitting the experimental data to this equation, and by comparing the fitted parameters with respective literature values. However, examination of eqn (3) shows that only two parameters (T_o and τ) can be varied independently. Moreover, the fitting process is not orthogonal in these two parameters, i.e., the effects of changing one parameter can be compensated by changing the other. This creates lack of orthogonality, i.e., numerical problems of slow convergence and a large scatter in the fitted parameters.

We reduced this problem somewhat by rewriting eqn (3) in terms of two new parameters C_1 and C_2:

$$T_{sur}(t) = C_1\sqrt{t} - C_2(1 - e^{t/\tau} erfc\sqrt{t/\tau}) \qquad (4)$$

$$\tau = \frac{4}{\pi}\left[\frac{C_2}{C_1}\right]^2$$

$$C_1 = \frac{2 I_o T}{\sqrt{\pi k \rho C}}$$

$$C_2 = \frac{I_o T L}{k}.$$

For the irradiation conditions in this study, the second term in the right side of Eq. (4) becomes very small after about 1 s, which allows a more reliable determination of C_1. We fitted the temperature-time data to Eq. (4) using a Nelder-Mead routine (function FMINS in Matlab[§§]).

[§§] The MathWorks, 24 Prime Park Way, Natick, MA 01760-1500.

RESULTS

Thresholds for pain

The average power density for all subjects (± s.e.m.) at 94 GHz required to evoke a threshold sensation of pain was 1.25 ± .05 W cm^{-2} for a 3 s exposure. This corresponds to a mean increase in surface temperature of 9.9°C from an average baseline (pre-exposure) temperature of 34.0 ± 0.2°C to an average final threshold temperature of 43.9 ± 0.5°C at the end of 3 s.

Thermographic data

Fig. 4 shows the average increases in skin temperature at each power density for all the subjects (points). The curves in Fig. 4 represent the results of the model (eqn 4 calculated using the averaged values for C_1 and C_2 given above). The model, with these two parameters, does an excellent job of fitting most of the data. However, systematic departures between the data and model at the lowest and highest exposures indicate that other small effects (such as loss of heat from skin to space) may contribute in a minor way to the observations. The fitted parameters for eqn (4), averaged from individual fits of the entire data set of all trials, were $C_1 \cdot I_o^{-1} = 5.5 \pm 0.5$°K cm^2 $s^{-1/2}$ W^{-1} and $C_2 \cdot I_o^{-1} = 2.5 \pm 0.8$°K cm^2 W^{-1} (mean ± SD).

A representative surface plot of the IR thermographic profile of the irradiated skin of a subject's back is shown in Fig. 5. The values for skin heating represent the temperature change [T_{sk} (3 s) − T_{sk} (baseline)] expressed as a percentage of the peak T_{sk} (3 s).

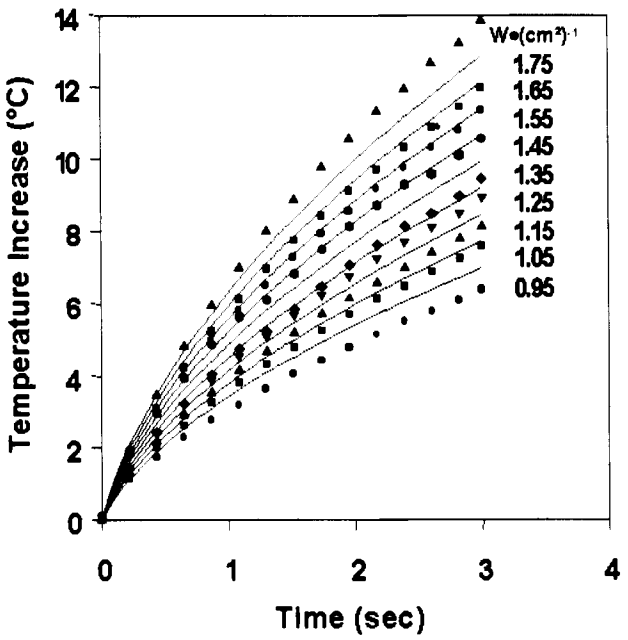

Fig. 4. The mean increase in skin temperature (markers) vs. fitted functions (curves) for a range of power densities (eqn 3).

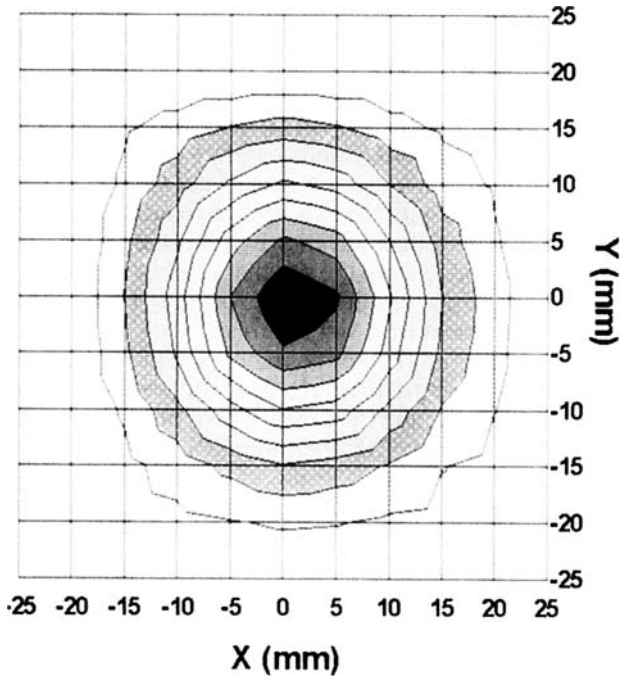

Fig. 5. Surface plot of the IR thermographic data from a single subject. The data represent the relative increase in temperature during the 3 s exposure (1.25 W cm^{-2}), where the central area represents 91–100% of the peak rate of temperature increase, and concentric circles indicate progressive 10% decrements in the rate of temperature increase.

DISCUSSION

Experimental data

Limited threshold data are available for both thermal perception and pain during exposure to microwave frequencies above 10 GHz. This is the first report of the pain threshold in human subjects undergoing microwave irradiation at 94 GHz. The pain threshold we report, expressed in terms of skin temperature, is similar to those reported by Hardy et al. (1952) for IR induced pain measured at similar locations on the back (42.2°C – 43.8°C, depending on the specific location on the back).

Cook (1952a) reported thresholds for pain stimulated by RFR at 3 GHz. Those data indicate threshold surface temperatures for pain that are 1–4°C higher than those reported by Hardy et al. (1952) for IR irradiation. This discrepancy cannot be explained as arising from differences in penetration depth between 3 and 94 GHz microwaves and infrared radiation, because in all cases the increase of the surface temperature was measured, and the thermal sensors are located near the surface of the skin. However, Cook (1952a) did not examine the same sites as those examined in the present investigation and he also used thermistors at discrete skin loci. As we discuss below, there are other indications of experimental error in Cook's study, perhaps from imprecise dosimetry.

Our investigation also differs from earlier studies in its use of IR thermography to measure the change in

surface temperature. This method offers at least three advantages: 1) temperature measurements are recorded in real time, by a system with fast effective response time, thus eliminating any temporal error due to the finite response time of thermistors or thermocouples; 2) the sensor array of the IR camera allows the simultaneous sampling of multiple discrete areas, and (3) no sensor is placed in contact with the skin, which reduces the chance of artifact. This latter advantage assures that measurements are obtained from the site that reaches the maximal temperature, thus eliminating error due to less-than-optimal placement of a single probe.

The utility of IR thermography for measuring skin temperature during RF irradiation can best be appreciated by comparing the field map shown in Fig. 1 with the surface plot of the IR thermographic profile of the irradiated skin surface of a subject's back shown in Fig. 5. In addition to providing accurate values for the temperature of the skin, it also provides an image of the beam's profile. As expected, the field map shown in Fig. 1 is very similar to the surface plot of skin temperature in Fig. 5. This similarity demonstrates the lack of appreciable heat conduction in a direction parallel to the surface of the skin, and supports the use of a one-dimensional thermal model.

There are no data on the threshold for thermal injury in response to mm-wave irradiation of animal or human skin. Hot water was used in the classic study of Moritz and Henriques (1947) to examine the relationship between T_{sk} and thermal exposure duration. If we extrapolate from their data, we find that T_{sk} must be maintained at approximately 68°C for 3 s in order to induce partial thickness burns. The mean T_{sk} of our subjects was 43.9 ± 0.5°C at the end of 3 s. This is far below the threshold for thermal injury. Furthermore, the exposure duration referred to in the work of Moritz and Henriques pertains to the duration of time at a given T_{sk}. In our investigation, the T_{sk} corresponding to the threshold of pain was the peak T_{sk} during any given exposure. It is therefore reasonable to suggest that individuals accidentally exposed to mm-waves, under the conditions examined in this investigation, would detect the painful stimulus and self-limit the exposure by moving away from the field, well in advance of sustaining any thermal injury. An extensive treatment on this issue is presented by Ryan et al. (2000).

Thermal modeling

We recognize that the microwave exposure required to induce threshold pain will vary with the initial temperature of the skin. However, under the thermally neutral conditions examined in the present investigation, the s.e.m. of the baseline skin temperature across subjects was only ± 0.3°C. Because skin temperature will vary under different environmental conditions, these thresholds must be regarded as approximate if extrapolated to different environmental conditions.

We first consider the agreement between the fitted parameters and those expected on the basis of literature values. Eqn (4) relates the fitted parameters C_1 and C_2 to thermal and electrical properties of tissue. The thermal properties of skin have been reported but are somewhat variable; by contrast, the electrical properties of skin are poorly established at 94 GHz (and undoubtedly are variable as well). We therefore use literature values for the thermal properties of skin and estimate the electrical properties from the data. In eqns (3)-(4) the thermal properties enter in the form of two groups of parameters:

$$\rho kC = 1.7 \times 10^6 \text{ W}^2 \text{ s/m}^4 \text{ °C}^2\text{(thermal inertia)}$$

$$k = 0.3 \text{ Wm}^{-1} \text{ °K}^{-1}\text{[thermal conductivity of skin,}$$

where the values cited are given for skin by Chato (1985)].

The electrical parameters are the energy penetration depth L and energy transmission coefficient T. These can be expressed in terms of the complex permittivity ϵ' of the tissue (a bulk property) by

$$T = 1 - \left| \frac{\sqrt{\epsilon'} - \sqrt{\epsilon_o}}{\sqrt{\epsilon'} + \sqrt{\epsilon_o}} \right|^2 \quad (5)$$

$$L = \left(\frac{-c}{4\pi f \, Im \sqrt{\epsilon'}} \right), \quad (6)$$

where the complex permittivity ϵ' is written as

$$\epsilon' = \epsilon_r \epsilon_o - \frac{j\sigma}{2\pi f}, \quad (7)$$

where ϵ_r is the relative permittivity, σ is the conductivity, f is the frequency, $j = \sqrt{-1}$, and ϵ_o is the permittivity of free space (a constant).

Fig. 6 shows the fitted values of L and T obtained from the data. The results show considerable variability. The means (± SD) of these parameters are 0.65 ± 0.08 for T and 0.16 ± 0.07 mm for L.

Few if any data exist for the complex permittivity of skin at 94 GHz from which these quantities can be independently calculated. Gabriel (1996) has summarized data extending to 10 GHz, and Gabriel provided empirical formulas by which to extrapolate the data to higher frequencies. This extrapolation yields a complex permittivity of 5.8–7.5j for dry skin at 94 GHz. Using these values leads to $T = 0.69$ and $L = 0.19$ mm, which agree well with the values obtained above from the curve fitting. We conclude that the simple model yields results consistent with reported values for the electrical and thermal properties of tissue. We note, however, that these properties are highly uncertain. Chato (1985) indicated a twofold range (0.21–0.41 W m^{-1} °K^{-1}) for the thermal conductivity of skin, and a similarly large range for the thermal inertia. The variability in the dielectric properties of skin at this high frequency is unknown but presumably also high.

The results in Fig. 6 show, in addition to considerable variability, a noticeable correlation between T and L. This correlation may arise from the fact that the thermal

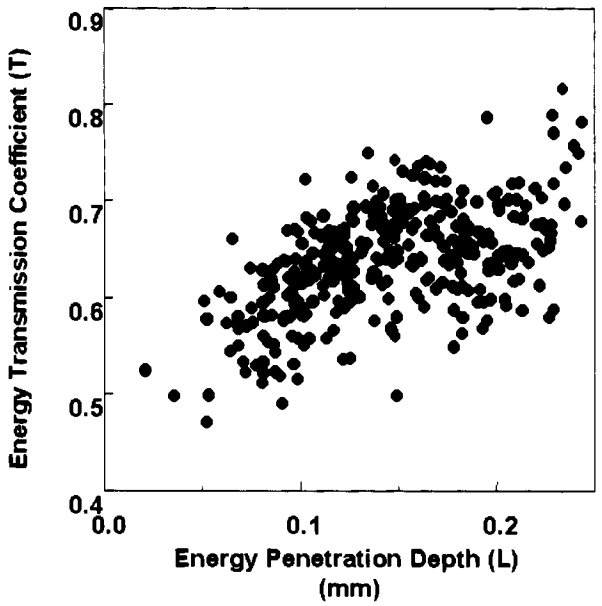

Fig. 6. Scatterplot of energy transmission coefficient, T, vs. energy penetration depth, L, obtained from fitting eqn (4) to the data.

and electrical properties of tissue depend strongly on water content. Increasing the skin moisture will increase the permittivity and electrical and thermal conductivity of tissue.

These results are in striking contrast to those of Cook (1952a), who deduced a thermal conductivity value for tissue of 2.1 W m^{-1} $°K^{-1}$ by fitting skin temperature data (using microwave heating at 3 GHz) to essentially the same theory that is presented here. This result is six to ten times higher than currently accepted values of thermal conductivity of skin and four times higher than for muscle or other soft tissues. However, these results may have been affected by experimental errors related to exposure assessment. Cook estimated the incident intensity of the radiation as the forward power in a waveguide placed against the skin, divided by the area of the waveguide. Because of the cosine distribution of the electric field in a waveguide, the exposure of the tissue beneath the waveguide is highly nonuniform, an important source of error. In the present study, the incident intensity and skin temperature were measured at the same location.

The model as described above is based on a single physical mechanism, thermal conduction from the skin into deeper layers of tissue. The model does not include convective cooling by blood flow, evaporative or radiative cooling of the surface of the skin, or various thermoregulatory responses of the body. These factors need to be considered when attempting to extrapolate the present results to other exposure conditions, particularly for substantially longer irradiation times. We consider the possible influence of other heat transport mechanisms.

Convective cooling by blood. A significant heat transport mechanism in tissue is convective cooling by blood flow. The amount of heat lost from the surface of the skin (where the temperature measurements are made) can be estimated using the bioheat equation, which is an extension of eqn (1) to include a term representing convective cooling by blood:

$$k\nabla^2 T(x, t) - \rho^2 C m_b[T(x, t)] - T_{core} + Q(x, t) = \rho C \frac{\partial T(x, t)}{\partial t}. \quad (8)$$

In eqn (8), m_b is the blood perfusion rate (typically 10 cm^3 100 g^{-1} min^{-1}) and T_{core} is the temperature of the blood in major vessels. (The specific heat and density of blood are assumed equal to those of other soft tissues.)

The solution of eqn (8) for microwave heating of tissue, and some comments on the validity of the equation, are presented elsewhere (Foster et al. 1998). In response to microwave irradiation such as considered here (eqn 2), the increase in the temperature of the skin is characterized by two time constants:

$$\tau_1 = \frac{1}{m_b \rho}(\text{convection})$$
$$\tau_2 = \frac{\rho C L^2}{k}(\text{conduction}). \quad (9)$$

With the parameter values deduced above (L = 0.16 mm, k = 0.3 W m^{-1} $°K^{-1}$, mb = 10 cm^3 100 g^{-1} min^{-1}), the time constants τ_1 and τ_2 are 600 and 0.3 s, respectively.

Detailed analysis of the theory (Foster et al. 1998) shows that, at short times, the heat transport in the tissue is characterized by heat conduction, and eqn (3) applies. At longer times ($>\tau_1$), convective cooling by blood dominates. Between τ_1 and τ_2 there is a gradual transition from conduction-limited to convection-limited heating behavior. Below an "effective" time of about 15 s (for the irradiation conditions considered here), the increase in surface temperature is nearly independent of the blood perfusion.

This behavior has a simple qualitative explanation. For short exposure times the temperature increase is confined to tissue depths of the order of L, and the temperature gradients near the surface of the skin are quite large. This causes the heat conduction term (the first term) in eqn (8) to dominate the heat transfer. As time goes on, heat diffuses more deeply into tissue, thermal gradients near the surface of the skin become smaller, and the blood flow term (second term) becomes more significant.

We conclude that the simplified equation (eqn 3) should be useful for exposure times somewhat greater than 10 s, particularly for the millimeter wave frequencies considered here. At longer times, effects of blood flow will become increasingly more noticeable.

Loss of heat from the surface of the skin into space. Eqn (3) was derived assuming insulated boundary conditions, i.e., no heat loss from the skin into space. In reality, heat loss from the skin, by convective cooling by air flow or by radiation from the surface of the skin into space), is a significant factor in the thermal balance of the body.

The amount of energy that will be lost from the skin into space can be estimated from modeling studies of Stolwijk and Hardy (1977). For a nude man in a thermally neutral environment with low air flow rates, these authors cite a heat transfer coefficient (combining both radiative and convective cooling) of 6.9 W m^{-2} $°C^{-1}$. This implies, for the maximum increase in skin temperature in the present study (<15–20°C above ambient room temperature) and modest air velocities (3 m s^{-1}), a heat loss from skin into space of the order of 100 W m^{-2}, which is roughly 1% of the incident microwave energy density. Thus, in the present experiments, the assumption of insulated boundary conditions is reasonable.

However, there are small systematic departures of the data from the model at highest and lowest exposure levels (Fig. 4). These suggests the presence of small effects that are not taken into account in the model, possibly heat transfer mechanisms other than simple conduction. However, the data in Fig. 4 are averaged over several subjects, not all of whom received all of the exposures indicated in the figure, and the departure may also reflect inter-subject variability as well.

Physiological (thermoregulatory) responses. As time progresses, the microwave exposure will elicit thermoregulatory responses, including increases in skin blood flow and sweat rate. However, in the short observation times in the present study, which are much shorter than the physiological response times, no thermoregulatory responses are expected.

Other considerations. Both eqns (1) and (8) assume a "continuum," i.e., a homogeneous tissue. In reality, the skin (as other tissues) is highly nonuniform. Lin et al. (1999) have recently considered instantaneous heating of the skin (to model laser injuries) using a model that takes into account heat propagation effects in different layers of skin. This model, which is mathematically complex, can provide more detailed information about skin heating over short times than the simplified model considered here. However, the present data are fitted quite well by the simple model and do not indicate the need for a more refined analysis.

We extended the model slightly to estimate the thresholds for thermal pain from exposures at different durations. Based on the present data (collected under thermally neutral conditions), we can assume that the threshold for thermal pain corresponds to a 10°C increase above normal skin temperature. Thus we can use eqn (4) to estimate the intensity of exposure needed to produce this temperature increase over different exposure periods.

Fig. 7 shows a cumulative distribution of calculated thresholds, based on the entire data set from the 10 subjects. The thresholds were calculated using the thermal model so as to produce a 10°C temperature increase during the assumed exposure time. This leads to median thresholds for painful heating of 3.2, 1.5, and 0.7 W cm^{-2} for exposures of 1, 3, and 10 s, respectively. We note that the thresholds are variable, even in the same subject, presumably due to variability in the electrical and thermal properties of the skin. In a general population under more diverse exposure conditions, the variability would presumably be much higher. The model can be readily extended to predict thresholds for pain at different frequencies, by using appropriate values for the dielectric properties of the skin. We defer that until a later study when data are available.

CONCLUSION

This study reports the thresholds for painful cutaneous sensation during stimulation by millimeter-wavelength microwaves, together with an analysis of the thermal response of skin in terms of a simple heat-conduction model. The data are in good agreement with the thermal model, with parameter values that agree well with those that have been reported in the literature. The model may provide a basis for estimating the thresholds for pain and for perception of microwave energy over a large range of frequencies and exposure times.

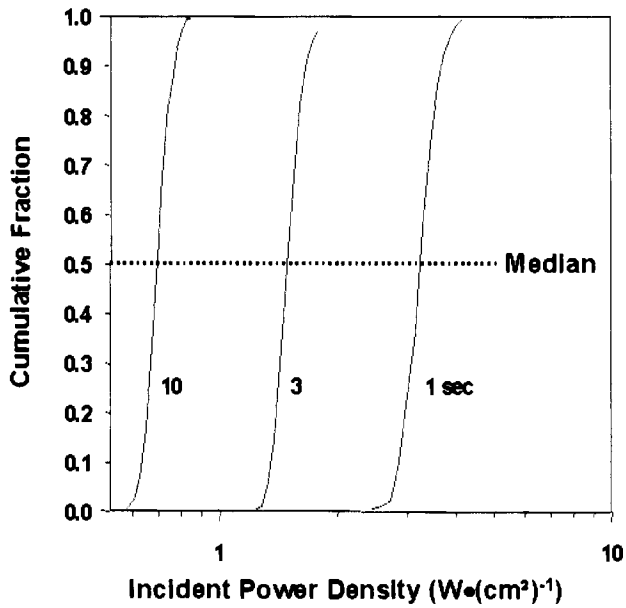

Fig. 7. Cumulative distribution functions of calculated thresholds for painful stimulation from exposure to 94 GHz microwaves at different exposure times. The thresholds were calculated using eqn (4), assuming a 10°C increase in skin temperature for each exposure duration. The distributions were generated by repeating the calculations for each set of parameters obtained by separately fitting all data from the measured thermal responses in the 10 subjects.

REFERENCES

Blick, D. W.; Adair, E. R.; Hurt, W. D.; Sherry, C. J.; Walters, T. J.; Merritt, J. H. Thresholds of microwave-evoked warmth sensations in human skin. Bioelectromagnetics 18:403–409; 1997.

Chato, J. C. Selected thermophysical properties of biological materials. In: Shitzer, A.; Eberhart, R. C., eds. Heat transfer in medicine and biology. New York: Plenum Press; 1985.

Cook, H. F. A physical investigation of heat production in human tissues when exposed to microwaves. British J. Applied Phys. 3:1–6; 1952a.

Cook, H. F. The pain threshold for microwave and infra-red radiations. J. Physiol. Lond. 118:1–11; 1952b.

Cornsweet, T. N. The staircase-method in psychophysics. Am. J. Psychol. 75:485–491; 1962.

Foster, K. R.; Lozano-Nieto, A.; Riu, P. S.; Ely, T. S. Heating of tissue by microwaves: a model analysis. Bioelectromagnetics 19:420–428; 1998.

Gabriel, C. Compilation of the dielectric properties of body tissues at RF and microwave frequencies. Brooks Air Force Base, TX: U.S. Air Force Armstrong Laboratory; Technical Report AL/OE-TR-1996-0037; 1996.

Hardy, J. D.; Wolff, H. G.; Goodell, H. Pain sensations and reactions. Baltimore: Williams and Wilkins; 1952.

Lin, J.; Chen, X.; Xu, L. X. New thermal wave aspects on burn evaluation of skin subjected to instantaneous heating. IEEE Trans. Biomed. Eng. 46:420–428; 1999.

Moritz, A. R.; Henriques, F. C. Studies of thermal injury II. The relative importance of time and surface temperature in the causation of cutaneous burns. Am. J. Path. 23:695–720; 1947.

Ryan, K. L.; D'Andrea, J. A.; Jauchem, J. R.; Mason, P. A. Radio frequency radiation of millimeter wave length: Potential occupational safety issues relating to surface heating. Health Phys. 78:170–181; 2000.

Riu, P. J.; Foster, K. R.; Blick, D. W.; Adair, E. R. A thermal model for human thresholds of microwave-evoked warmth sensations. Bioelectromagnetics 18:578–583; 1997.

Shelton, W. W. Millimeter-wave exposure system augmentation. Brooks AFB, TX: U.S. Air Force Armstrong Laboratory; Technical Report AL-TR-1991-0056; 1991.

Simpson, W. A. The step method: A new adaptive psychophysical procedure. Percept. Psychophys. 45:572–576; 1989.

Stolwijk, J. A. J.; Hardy, J. D. Control of body temperature. In: Douglas, H. K., ed. Handbook of physiology, section 9, reactions to environmental agents. Bethesda, MD: American Physiological Society; 1977: 45–69.

Wetherill, G. B.; Levitt, H. Sequential estimation of points on a psychometric function. Brit. J. Math. Stat. Psychol. 18:1–10; 1965.

■ ■